ORIGINAL PAPER

Dynamic WAAM: adaptive processes for equivalent contact surface (ECS) optimization

Ethan Kerber[1,2] · Jan Luca Fahrendholz[1,2] · Sigrid Brell-Cokcan[1,2] · Peter Dewald[1,2] · Rahul Sharma[1,2] · Uwe Reisgen[1,2]

Abstract

Wire arc additive manufacturing (WAAM) integrates benefits of automation and mass customization to improve efficiency through near-net part production. While WAAM is well researched, there remain significant challenges as the complex relationship between robot, welder, and process parameters can lead to inaccuracy in geometry and variations in material properties. This research proposes a novel framework for quantifying the WAAM process and proposes dynamic adaptive strategies for improving production. This paper introduces the concept of an equivalent contact surface (ECS) for quantifying the additive welding process. Adaptive methods are then identified to optimize WAAM production. In conclusion, this paper provides an outlook on future research directions for continuing the development of this dynamic WAAM process.

Keywords Wire arc additive manufacturing · WAAM · Dynamic · Adaptive · Robotics · Optimization · Welding · Equivalent contact surface

1 Introduction

Additive manufacturing (AM) is characterized by the successive application of melted materials including; paste-like, powder, liquid, thermoplastics, or metals (DIN 2016). The ISO/ASTM52900 differentiates seven types of AM according to their method of material application and cohesion process (Technology of Materials Standards 2017). For

✉ Ethan Kerber
  kerber@ip.rwth-aachen.de

  Jan Luca Fahrendholz
  fahrendholz@ip.rwth-aachen.de

  Sigrid Brell-Cokcan
  brell-cokcan@ip.rwth-aachen.de

  Peter Dewald
  peter.dewald@isf.rwth-aachen.de

  Rahul Sharma
  sharma@isf.rwth-aachen.de

  Uwe Reisgen
  office@isf.rwth-aachen.de

1   RWTH, Chair for Individualized Production (IP), Campus-Boulevard 30, Aachen 52074, NRW, Germany

2   RWTH, Welding and Joining Institute (ISF), Pontstraße 49, Aachen 52062, NRW, Germany

large-scale applications such as construction, an additive manufacturing process must be capable of producing large parts quickly and cost-effectively, with a resulting high strength-to-weight ratio and medium to fine surface quality and complexity. Compared to traditional primary forming processes such as milling, molding, or extrusion, AM is characterized by its ability to rapidly mass customize design options. Whereas milling must remove substantial material to reach the final geometry, AM prints parts near their final form. While molding and extrusion achieve efficiency through standardization and multiple re-use of formwork, AM achieves efficiency through customization, as individualized production can be achieved faster and without significant tooling changes. As such, the additive process enables a new form of digital manufacturing with a new set of process constraints to be optimized.

As a type of additive manufacturing, directed energy deposition (DED) and its specific subset, wire arc additive manufacturing (WAAM), is advanced enough to be well suited for industrial application and capable of fulfilling construction scale requirements. However, the resulting structures still need to manage process parameters and production constraints to achieve specified performance in terms of geometric tolerances and material properties.

In the WAAM process, geometry is built through material deposition. This is achieved through the robotic manipulation of welding torches already commonly used in industrial manufacturing. While this allows for the production of large parts, overhangs must be taken into account as there is generally no support structure. When welding overhangs, the effect of heat and gravity make the process challenging as the molten metal may not adhere to the printed object without deformation or failure. The challenges of overhang welding can be overcome by incorporating a rotary axis into the robotic cell so that the weld can always be applied in the optimum orientation where the welder is vertical in the Z axis and the built upon layer is perpendicular in orientation to the torch. The trade off of achieving this orientation through the use of a rotary axis is the new constraints of the positioner which can limit the possible size of production. If the ability to print overhangs can be achieved without a rotary axis, then the limitations on the size of the printed object, normally determined by the reach-ability of the robot, can be extended by adding one or more external linear axes. With these robotic extensions, the build area of AM processes can enable even larger scale production of components for use in architecture, engineering and construction.

The diversity of materials that can be welded, enables WAAM to create parts in a wide range of specifications with regards to production properties and material performance. However, welding has additional limitations that must be considered. The heat transferred during the welding process results in material properties that affect the performance of the structure.

The research represented in this paper is a collaboration between RWTH Aachen University Institutes; the Chair for Individualized Production (IP) and Welding and Joining Institute (ISF). Research in WAAM is conducted at both institutes with the IP WAAM cell consisting of a KUKA KR 30 robot with Lorch GMAW torch connected via the Cloud Remote Control Framework developed by Robots in Architecture Research. Process monitoring is accomplished by a Optris XI 400 thermal camera. The WAAM research cell at the Chair for Individualized Production is shown in Fig. 1. Research in WAAM conducted at the ISF consists of a linear Axis driven Fronius CMT welder also assisted in process monitoring by an Optris thermal camera.

In all application scenarios, it is important to integrate the consideration and optimization of constraints as parameters in the earliest design stages. The interrelation between process parameters, material properties, object geometry and thermal dynamics all combine to affect the structural nature of the final WAAM object. Among these influences, the rate of thermal heating and cooling resulting from the energy transfer of the welding process plays a significant role in determining the strength and hardness of the final object. The effect of heat transfer impacts the material build-up and the final state of the part geometry.

At all levels of production, it is vital to ensure the specified structural performance of the production part, as failure can result in significant damage or injury. A key aspect of structural performance is the material properties. It is crucial to understand the impact of process parameters on material hardness and strength. This requires a refined understanding

Fig. 1 WAAM research cell at the Chair for Individualized Production RWTH Aachen University

of thermal dynamics in WAAM. This paper explains a novel concept of an Equivalent Contact Surface (ECS), which is created to represent the relationship between energy transfer during the welding process, the resulting heat accumulation and distribution during cooling, and the resulting impact on material geometry, hardness and strength.

Using the ECS as an abstract representation of the impact of thermal dynamics, this paper proposes adaptive strategies to improve the WAAM outcome and enable the production of parts with complex geometries, including unsupported overhanging geometries. The following sections introduce the concept of the ECS and explain its representation of the relationship between thermal dynamics, process parameters and geometric characteristics.

2 Equivalent contact surface

This section introduces the idea of an auxiliary value model for heat dissipation during the WAAM process. The first part of this section explains the idea of the model, the motivation behind it and its usefulness. The influence of the main parameters on the heat accumulation and the geometry of the test specimen is then reviewed. This is followed by review of the state of the art in measuring these parameters and their effects on the weld. The next part will look at research into the limits of setting controllable parameters and the effects of going beyond these limits. Another aspect, which will be discussed in this section, is the anisotropy in WAAM and how it is affected by the aforementioned parameters. The equivalent contact surface concept is developed to inform adaptive processes to improve WAAM production.

In WAAM, the cooling rate has a major influence on the viscosity and surface tension of the molten pool, thus affecting the geometry of the specimen (Shi et al. 2018). The cooling rate also has a direct impact on the mechanical properties by effecting grain growth and phase transformations (Reisgen et al. 2020). Cooling rates are dependent on the ability of the structure to dissipate the heat introduced and accumulated during the welding process.

There are two methods by which heat is released from the WAAM object during production. Conduction dissipates heat into the base material and lower layers of the printed object. Convection & radiation dissipates heat by releasing it into the atmosphere through the surface of the printed object. (Fig. 2). Heat dissipation by this convection & radiation, where the accumulated heat is released through the material surface exposed to the air, is less effective than heat dissipation by conduction, where the accumulated heat is released through the base material and built up layers.

Due to the reduced effectiveness of convection and radiation, heat dissipation decreases with increasing layer height (Shi et al. 2018). This means that the more mass the WAAM
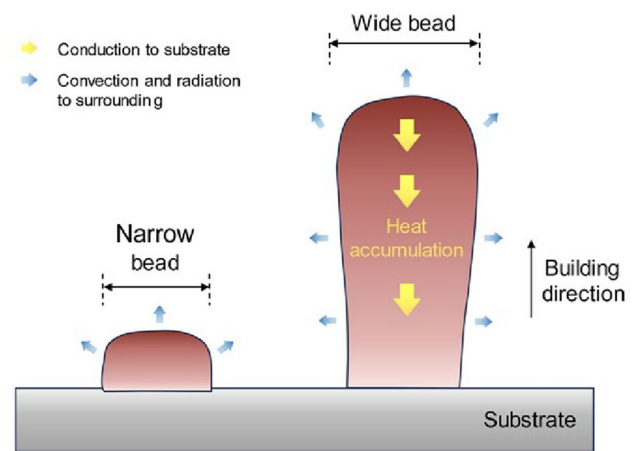

Fig. 2 Heat dissipation dependency on build height (Wu et al. 2019)

object has, the longer it will retain heat. It also means that as the print grows, it will retain more and more heat, as the increase in surface area has less effect on heat dissipation than the increasing mass of the object has on heat retention.

This is important to consider when designing WAAM processes as the impact of different cooling rates will impact the strength and hardness of the material as well as the geometric buildup of subsequent layers and the ability to print overhanging forms without support structures. For example, if the wait time between layers is set to a constant value, but the mass of the surface changes, the cooling ratio will change and the heat of the layer to be printed on will also be different. This will lead to variations in the material microstructure and the resulting strength and hardness properties, as well as unwanted effects in the resulting printed geometry.

The hotter the base layer, the more the subsequent layer will absorb into it, resulting in a lower layer height and affecting the quality of the continued path planning if adaptation is not integrated. The layer height and width will be either too low or too wide if the layer printed on is too hot. On the other end of the spectrum is the opposite effect, where the printed layer will be too high and narrow if the printed-on layer is too cold. The heat transfer during the WAAM process leads to changes in the heat affected zone which impact the microstructure properties of the metal and subsequent hardness and strength that results depending on cooling rates.

Hardness is a result of the phases present in the microstructure of the deposited material. These phases are the result of the ability of the metal's atoms to rearrange themselves in an ordered fashion as the material cools from a molten state. Rapid cooling leads to a harder, more brittle material as the atoms are unable to arrange themselves in an ordered fashion, resulting in a metastable phase called "martensite". This phase is hard and brittle with a microstructure that looks like needles or plates. The hard but brittle material

property of steel is often intended when the metal is to be used in tools or wear resistant structures. However, this brittleness can also result in increased cracking or distortion. Slow cooling leads to a softer, less brittle material as the atoms are able to arrange themselves in an ordered fashion, resulting in pearlite phases. Pearlite can be described as a microstructure with layers alternating between ferrite (less dense molecular structure) and cementite (denser molecular structure). These variations in cooling rates can range from highly rapid cooling at a rate of around 100°C/s or higher to low cooling rates measured as low as 10°C/s or lower. The challenge is that changes in cooling rates between printed sections of WAAM structures can lead to undesirable microstructure variations and faults in the material, resulting in fatigue or cracking.

The geometry and structural properties of the material (strength and hardness), the cooling rate and therefore the geometrical and mechanical properties are also dependent on the interlayer dwell time, the cooling method and the surrounding temperature (Wu et al. 2019). The influence of the geometry

on the accumulated heat within the specimen can be seen in Fig. 3. Here two half circle wall structures have been welded with the same parameters and the same set up. The wall on the left picture has a diameter of 4 cm and the structure on the right side a diameter of 8 cm. To determine the thermal cycles of the welds a thermometric camera was used to record the temperature of the inner side of the walls. Then 3 areas were defined for which the mean temperature over the time was determined. The 3 areas are located in the middle of the wall, whereas the first is located close to the base, the second one lies roughly in the middle of the height and the third is locates close to the top layer. The positions of the areas are located in the same places for both structures in regard to the welding and camera position. Between each layers a dwell time of 60 s was used. For the half circle with 4 cm diameter between the 20th and the 21st layer a longer dwell time occurred. Regarding the t8/5-times (the cooling times between 800 °C and 500 °C) differences between the two welds could be found. Area 1 has the most and the shortest t8/5-cycles for both structures. For the larger structure the heat accumulation was greater as the

Fig. 3 Thermal image and temperature over time of two half circle wall structures with a diameter of 4 cm (left) and 8 cm (right)—documentation of thermal effect
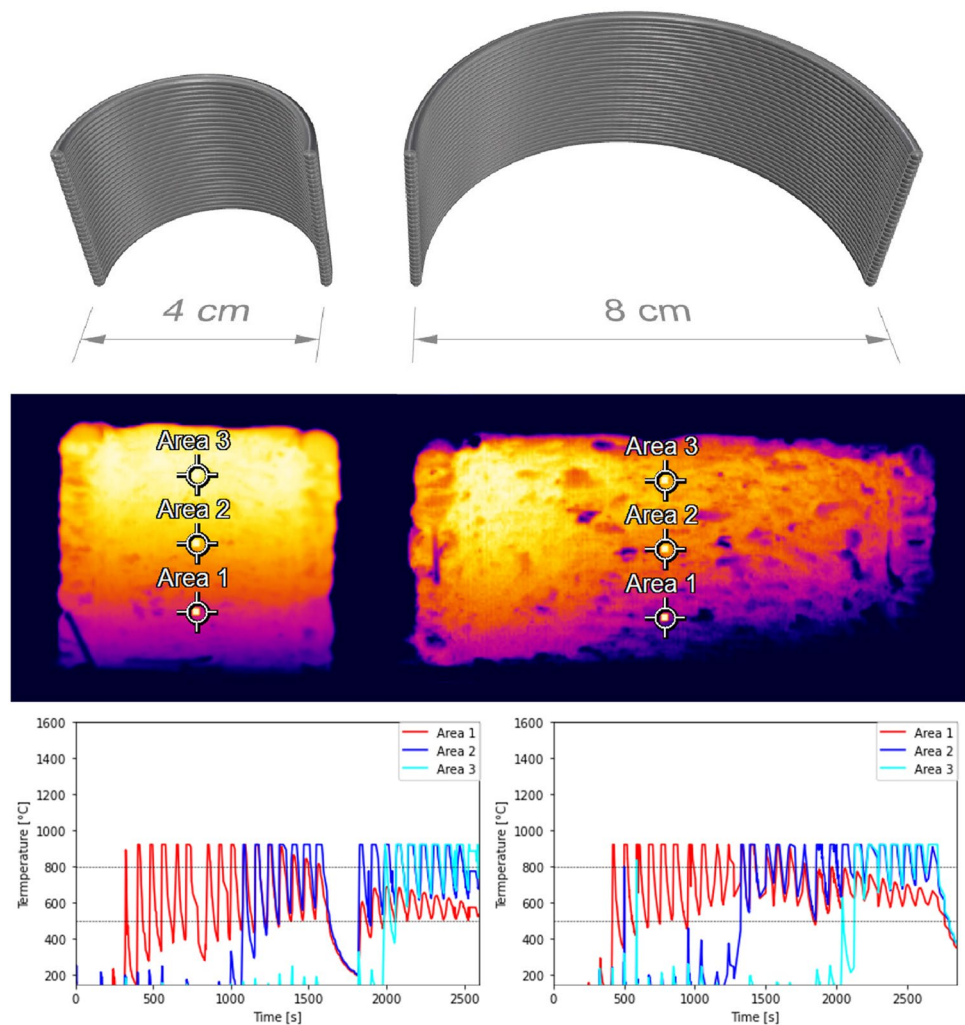
longer t8/5-times show. This is also evident in the temperature between layers. For the smaller structure the temperature drops lower between layers than for the bigger one. This means fewer t8/5-times for the big structure since the heat accumulates so much, that the temperature between layer deposition does not fall below 500 °C.

The temperature of the structure is monitored by an Optris XI 400 thermal camera with a range from -20 °C to 900 °C. While the temperature of the welding process does exceed this range, the cool down rate between 800 °C and 500 °C is able to be examined with this thermal camera. The cooling rate can be extracted from this information as the Optris camera has been IoT enabled to publish thermal data through a custom built python script to inform ECS investigations. In Fig. 3 it can be seen that due to a kinematic problem with the robot there was an excessive cooling time around timestamp 1700. The specimen remains included in the research's studies to examine the impact of this during destructive testing where material microstructure and inter-layer bonds are investigated.

To summarize the influences on the heat accumulation and dissipation, the idea of the ECS is introduced as an auxiliary variable. The ECS represents the summary of the boundary conditions affecting the heat transfer, considering the process parameters. In addition to the measurement of mass (conduction) in relation to surface area (convection), other parameters that influence this variable are welding power, position, speed and material properties. The ECS can be understood as a value that summarizes the heat dissipation of the produced part and gives a direct implication on the cooling rate of the weld. The idea is to use this auxiliary variable for an adaptive path planning, where the ECS is used to determine the optimal path to reduce differences in cooling ratios by dynamically adjusting the path planning to adjust the dwell time based on thermal measurements and achieve a more consistent cooling rate throughout the print.

The ECS must be determined considering gravitational effects. To investigate this impact, the parameter ranges will be studied under different welding positions. After modeling the ECS and investigating the influence of the welding position, correlations between the auxiliary variable and the mechanical properties, as well as its anisotropy, shall be determined. The heat transfer parameters to be investigated in relation to the ECS and their effect on geometry, surface roughness and mechanical properties, as well as the measurement methods used in WAAM to determine them, are discussed in the following Sect. 2.1.

2.1 Influences on heat accumulation, geometry, and surface texture

As the heat level within the specimen has a major influence on the cooling rate of the molten pool, the predominant heat input factors, wire feed and the welding speed, have a major influence on the heat accumulation within the workpiece (Schroepfer et al. 2021). Research (Dinovitzer et al. 2019) shows the effects of the wire feed rate and welding speed on the bead geometry. It is shown that the wire feed rate has a proportional influence on the height of the bead, but not on its roughness.

It has also been observed that as the travel speed increases, the bead width decreases and its roughness increases. In terms of bead width, the same behavior was observed for wire feed and welding speed (Schroepfer et al. 2021). The gas flow rate had no effect on the geometry in the study by Dinovitzer et al. (2019). The influence of the shielding gas composition was investigated by Gurcik et al.. Their paper implies that a reduction in CO_2 content leads to an increase in surface quality. Also, it is suggested, that the usage of helium and CO_2 leads to a geometric deformation and a reduction in surface quality (Gurcik et al. 2019). This may result from changes within the arc condition due to the different properties of these gases.

Another controllable parameter that affects the energy per unit length and therefore the heat input is the voltage. It primarily determines the arc length and the width of the weld pool. Voltage, like current, also affect several other weld features such as residual stresses, arc stability and the droplet transfer mode (Anzehaee and Haeri 2011). In addition to the heat input, the preheat temperature of the specimen is also affected by the time elapsed between depositions, known as the dwell time. Other parameters affecting heat dissipation, such as active cooling and surrounding temperature, also influence the process (Reisgen et al. 2020). In addition to these process-specific parameters, path planning has a significant impact on heat accumulation and distribution.

Figure 4 shows the heat distribution for welding a spiral path in different directions. The figure on the left starts from the outside, welding towards the inside of the plate while the figure on the right starts from the inside and welds towards the outside of the plate. As the cross section shows, this has a direct effect on the heat affected zone (HAZ) and the microstructure of the welded part.

2.2 Measurement and detection systems for WAAM

Different measurement and detection systems are used in WAAM. An overview and revision of the applicable non-destructive testing (NDT) methods are given in Lopez et al. (2017). A selection of measuring signals used in WAAM is shown in Fig. 5. Online measurement systems in WAAM can be divided into offset and non-offset methods. Commonly used offset online measuring systems, which appraise the surface behind the molten pool, are laser sensors, CCD cameras, and infrared cameras. Non-offset online measurement systems require data related to the arc region and appraise
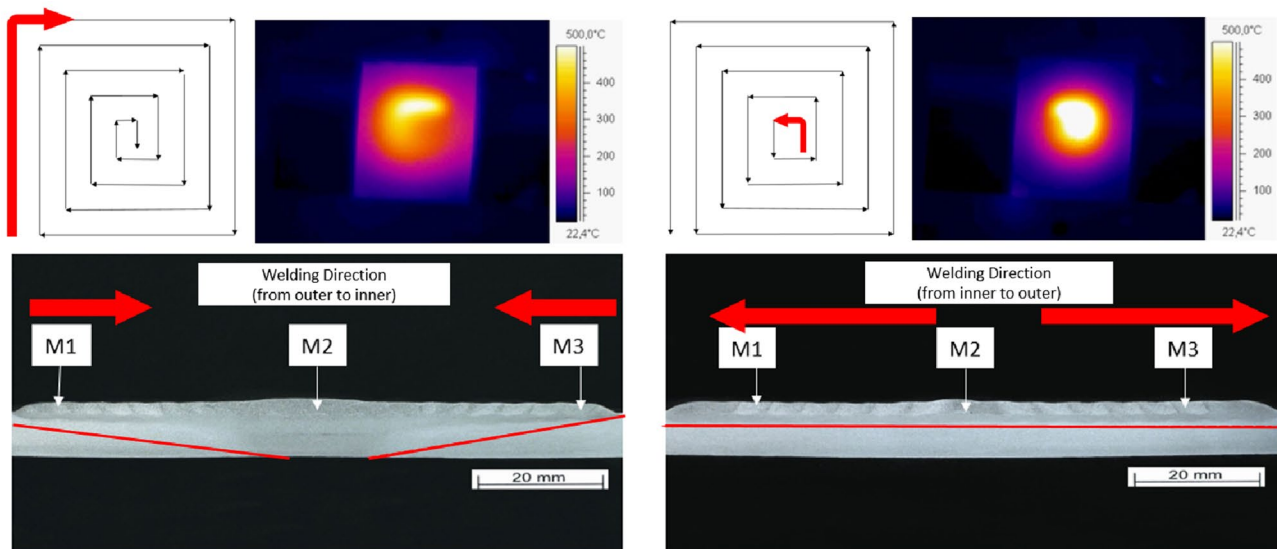
Fig. 4 Heat distribution for welding inwards (left) and outwards (right)
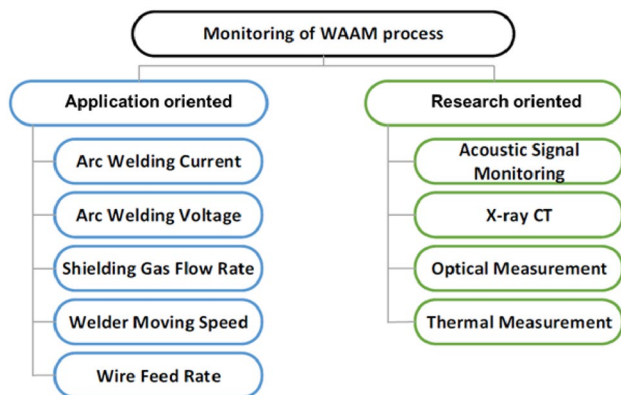

Fig. 5 Methods for monitoring of WAAM processes(Xu et al. 2018)

the molten area directly. CCD cameras and infrared cameras are also commonly used for this type of measurement system (Wang et al. 2020).

Richter et al. used a camera system for online measurement of the molten geometry. The system measured a temperature for each pixel of the image, which was then compared to the liquid temperature of the material. Pixels with a higher temperature were then assigned a Boolean true state to determine the geometric parameters of the molten pool (Richter et al. 2021). Acoustic signal measurement is also a viable method for online process monitoring. Tang et al. investigated the relationship between acoustic signals during Gas Tungsten Arc (GTA) WAAM and arc length. This research claims the possibility of arc length control through acoustic signal processing (Tang et al. 2022). Hallam et al. use a range resolved interferometry instrument to monitor

the layer height in-process. Their research compares the in-process measurements with micrometer measurements taken after each layer deposition and laser scanning measurements of the finished specimen, which shows an accuracy less than 0.005 mm (Hallam et al. 2022).

A common method for post-process measurement of the surface and geometric accuracy of the build is the use of optical 3D scanners of different measurement principles, as used by Wang et al. (2022) for height measurements of the deposited layers.

2.3 Determination of parameter space

In WAAM, different parametric limits can be determined depending on how the process is set up. As a result, commonly used ranges for parameter settings (parameter spaces) can be found. With regard to the used material and process setup, the interlayer temperature is often kept between 50 and 120 °C (Reisgen et al. 2020). For the gas metal arc welding process (GMAW), commonly used parameter ranges are wire feed speeds between 2 and 8 m/min and travel speeds between 0.2 and 1.2 m/min. Current and voltage are highly dependent on the arc mode and can range from 50 to 200 A and 10 V–30 V respectively.

For the gas tungsten arc welding process (GTAW), the wire feed speed is usually around 0.2 m/min and 1.5 m/min, and the travel speed is around 0.08 and 0.24 m/min. Typical wire diameters are 1.0 mm and 1.2 mm. Controlled short arc and pulsed processes are commonly used in WAAM applications. In the current research we utilize GMAW with steel wire 1 mm width and a wire feed speed of between 2 and 5 m per minute. During ECS experiments an ideal ratio was

found to be 5 m/min WFS to 0.36 m/min robot tcp travel speed. Experiments are ongoing with regards to dynamic wire feed speeds as well as weaving and oscillation based robotic path planning to study the impact of travel speeds and torch positions. The influence of the torch angles and welding direction on the GMAW process has been investigated by Su and Chen (2019). Their research shows that when both angles are 90°,the process has deeper penetration, fewer defects such as undercutting or spatter, and is more stable, but the porosity of the welds was also higher (Su and Chen 2019). The gas flow rates used in the papers reviewed ranged from 10 to 25 l/min. The shielding gases used in the literature were generally mixed compositions of argon and CO_2 for mild steel applications. Gurcik et al. also investigated the influence of helium and oxygen content. For non-iron based alloys, such as the aluminum-based alloy Al-5356 and the nickel based alloy Inconel 625, the shielding gases are mostly pure argon gases (Gurcik et al. 2019). Jurié et al. investigated the influence of different shielding gas contents such as CO_2 and H_2 on Inconel 625. Their study suggests an increase in hardness and tensile strength, but also higher surface waviness for CO_2 contents within the shielding gas (Jurié et al. 2019).

The welding position in relation to the gravitational influence was investigated by Penney et al. using a tilted building plate and varying torch angles. For a thin-walled square built on a 45° tilted base plate with a torch angle of 90° to the plate, the vertical sides of the square were bumpy and showed a high waviness. When welded downhill at a steeper torch angle of 50°, the vertical sides improved greatly while the horizontal sides became wavy and no longer perpendicular to the base plate. This paper has shown that it is possible to produce long thin-walled overhangs with angles up to 90° and more from a perpendicular thin-walled base. As the angle increased, the surface waviness on the underside also increased. Penney and Hamel (2019)

The most influential parameters of heat accumulation shall be summarized with respect to the equivalent contact area. The usable parameter space of the ECS will then be encoded into a computational model and investigated with respect to the welding position and the deposition rate, as shown schematically in Fig. 6. In this figure, the range of the surface area represents the welding position. This range represents the position of the torch from a space on the surface with the torch pointed towards the center of the space. The diameter of the surface represents the deposition rate of the material. The graphical representation of the ECS results in a visual calculation of the usable parameter space that results in WAAM settings that achieve the intended material properties in terms to strength, hardness and geometry build-up. This preliminary visualization will be populated with test data as parameter tests are conducted in later stages to add more quantitative results to this current preliminary visualization.

While the parameter space needs to be investigated under different welding positions, it can be assumed, that welding positions close to the overhead position will result in smaller usable parameter ranges than positions close to a flat position.

This is illustrated by the following weldment in Fig. 7. Here a wall was welded under a 90° angle in a horizontal position. The welding speed and the wire feed speed were 0.45 m/min and 5.0 m/min respectively. The layers were welded with a dwell time of 60 s without active cooling.

For this weld a material loss of approximately 17% of the deposited material was observed due to droplet and spatter formation. In addition, the remaining droplets resulted in an extremely rough surface on the lower side of the wall. This shows, that high temperatures and insufficient cooling times can drastically limit the usable parameter space when welding in constrained positions. Here, the use of adaptive strategies informed by the ECS variable can help to adjust
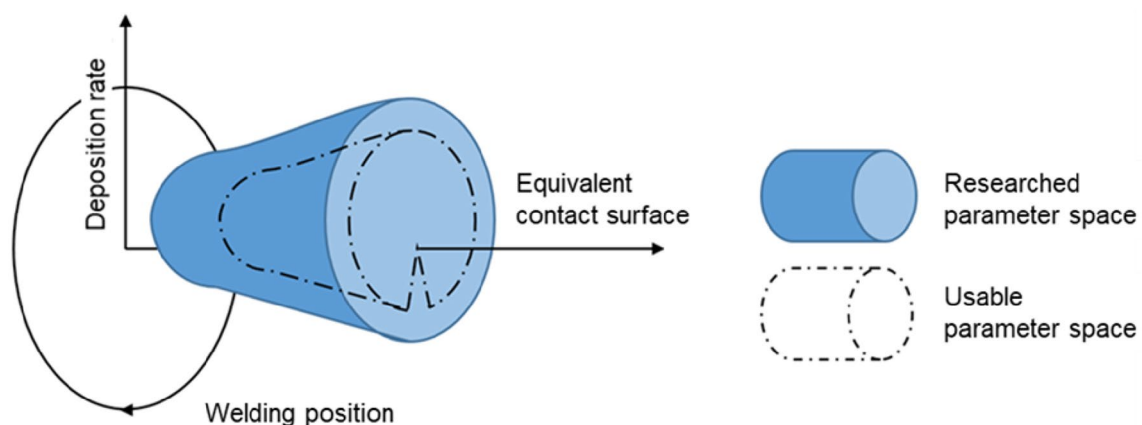

Fig. 6 Parameter space of the equivalent contact surface in terms of welding position and deposition rate

Fig. 7 Exemplary weldment at a 90° angle

the parameter settings and the path planning to increase the ability to weld with consistent thermal dynamics and achieve overhangs without support structures.

2.4 Influences on mechanical properties and anisotropy

WAAM manufactured components exhibit anisotropic mechanical properties where the structural material behavior is directionally dependent. The reason for these anisotropic mechanical properties lies in the local differences in the thermal profiles along the part. These lead to different phase transformations, grain sizes, and microstructures within the printed part, resulting in inhomogeneous material properties (Wu et al. 2019). Yildiz et al. investigated the influence of different process parameters on mechanical properties. According to their research, increasing heat input leads to a reduction in hardness (Yildiz et al. 2020). The study of Shassere et al. (2019) shows a decrease in impact toughness with increasing build height. This is determined to be due to the change in heat dissipation mechanism from conduction to convection as shown in Figure 10. As a previous study presented in Fig. 8 shows, the impact toughness is also dependent on the building direction.

Syed et al. investigated the influence of deposition strategies on fatigue crack growth in a titanium alloy produced by WAAM. They observed a difference in fatigue crack growth rate between crack growth parallel and perpendicular to the building direction (Syed et al. 2021). With regard to the fatigue load of WAAM manufactured austenitic stainless steel components, the work of Duraisamy et al. shows a higher fatigue strength at 2×10^6 cycles for specimens taken perpendicular to the building direction (Duraisamy et al. 2021). In terms of tensile strength, several studies show comparable strengths in welding and building direction, with the elongation of the material being dependent on the direction (Yildiz et al. 2020; Ghaffari et al. 2019). The mechanical properties, especially the tensile strength, of wire and arc additive manufactured components are often
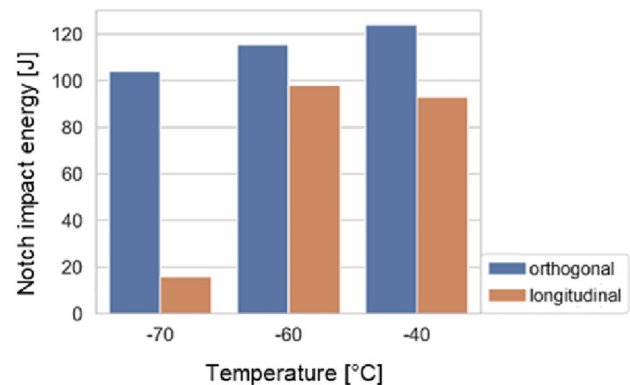

Fig. 8 Impact toughness over the temperature of a mild steel welded WAAM part

comparable to cast material (Wächter et al. 2020; Pan et al. 2018; van et al. 2020). For the aluminum alloy 5356, the investigation by Zhao et al. shows similar results for the anisotropy of tensile strength as for mild steel. The tensile strength parallel to the welding direction in their paper was about 13 % higher than orthogonal to the welding direction. Elongation was about 50 % higher in the welding direction (Zhao et al. 2022). Zhang et al. investigated the mechanical properties of Inconel 625. Their research also shows about 6 % higher tensile strength in the welding direction but about 20 % higher elongation orthogonal to it Chen et al. (2018). Zhang et al. also found the tensile strength to be greater and the elongation to be lower in samples taken in, compared to samples taken orthogonal to the welding direction for Inconel 625 (Zhang et al. 2022).

2.5 Modeling strategies in WAAM

In WAAM, modeling is often used to estimate weld quality, bead geometry, and mechanical properties, or to optimize the path planning process. The modeling can be performed using mesh-based methods, such as finite or boundary element methods, or using mesh-free methods

such as smoothed particle hydrodynamics (JSRSMSSO 2022). An example of geometry and microstructure modeling is given in Geng et al. (2021), where the authors use a finite element model coupled with a phase field model to investigate the thermal distribution and micro structure evolution of an aluminum alloy during WAAM.

Due to the high complexity of the welding process, artificial neural network approaches are often used for process modeling (Yaseer et al. 2021). Another often seen modeling approach is the use of a regression method, such as linear regression where an analysis model estimates the statistical relationship between a dependent variable, the response variable, independent variables, and the explanatory variables (Bingham and Fry 2010). Schröpfer et al. determined the correlation between welding parameters and variables in wire and arc additive manufacturing of high-strength steel using a regression analysis approach (Schroepfer et al. 2021). Lee uses a Gaussian process regression method to create a WAAM-process model for improving productivity and bead deposition quality. The Gaussian process regression is a non-parametric approach that calculates the probability distribution of all feasible data fitting functions (Lee 2020). Since regression analysis approaches are well fitted for determining correlations between process parameters in the WAAM process, they offer a good base of operations to model the equivalent contact surface.

The most influential welding parameters on the heat dissipation according to research are the travel and the wire feed speed, the voltage, and the dwell time. The most influential geometric and materialistic parameters are the printed volume, the surface of the print, and the heat conductivity and capacity respectively.

While the current paper establishes the ECS concept, the research is not yet able to quantitatively define the equation or relationship between the parameters that inform the ECS. To do this, follow up research will engage in parameter testing and material cross section analysis to establish the relationship between parameters and propose a more quantitative determination of the ECS.

Within the field of welding research, time-temperature-transformation diagrams (TTT-Diagrams) are widely established and generate a direct relation of cooling time to the phase transformation and the resulting mechanical properties for the corresponding metal. To determine the cooling times and relate the ECS to the mechanical properties of the weldments, aside from temperature measurements, the concept of TTT-Diagrams shall be reversed.

For this, weldments with the widely applied welding material G3Si1 according to DIN EN 440 will be utilized. From these, specimens are to be produced and exposed to varying thermal cycles to determine the resulting microstructure and hardness. With this a relation between thermal cycle and cooling time and the microstructure of the weld shall be established in diagram like a TTT-Diagram.

Then weldments with varying welding speeds, wire feed rates, volumes, surface areas and dwell times are to be produced. The resulting microstructure for these welds, as well as the hardness will be analyzed and from this, the influence on the welding parameters on the cooling time and microstructure is to be determined.

The framework of Equivalent Contact Surface (ECS) quantifies the parameter space of Wire Arc Additive Manufacturing allowing for a more thorough process model to be established. The goal of this research is to connect the ECS framework to the robotic welding process and inform adaptive strategies. The following section identifies areas where the ECS can dynamically inform adaptive approaches in WAAM.

3 Dynamic adaptation in the WAAM process

After establishing the concept of the Equivalent Contact Surface (ECS) the goal is to leverage this auxiliary variable to inform adaptive processes, improving the ability to achieve production with consistent thermal transfer / cooling cycles, and allowing for more capable WAAM production of support free overhanging geometry. This extends to both pre-planning of processes as well as in-line adaptations. The following section details adaptive strategies for an ECS informed WAAM process. This includes the creation of slicing algorithms for adaptive path planning, Internet of Things (IoT) enabled systems for online process control and the generation of WAAM information models (WIM) to capture data for analysis.

3.1 Slicing algorithms for adaptive path planning

The basis of WAAM tool path extraction from a 3D CAD model lies in the slicing strategy. Typical slicing algorithms utilize process parameters such as layer height, wall thickness, and infill strategies to create tool paths for printing. Strategies for slicing algorithms range from parallel to non-parallel, and from planar to non-planar to spatial. The goal of an adaptive slicing algorithm would be to integrate the ECS concept as a process parameter into the tool path pre-planning. This inclusion would generate early design decision analysis for path movement that is not limited to just execution of a path but capable of monitoring heat transfer and cooling cycles to adapt the movement of the robot or the parameters of the WAAM process. In pre-planning, this approach assesses the layer height and width, torch orientation, material overhang and estimates the amount of weld that can be applied to achieve an ideal heat affected area. The difference between traditional and the adaptive path

planning is that where a standard slicing algorithm defines a list of frames for the robot TCP to move through without sensor input, the adaptive algorithm can execute material deposition while monitoring thermal cooling cycles, to adapt the robot's path in an effort to maintain consistent thermal dynamics. This functions by dynamically sorting through the layer information during the process, adding the thermal information as metadata to points already executed on the print, and when a temperature threshold is crossed, adapting the path to print on a section of the structure that is already cool enough to receive further welds. This dynamic monitoring of thermal data then tracks the heat affected zone and informs the adaptive path planning when the cooling cycles are at a level where further material can be deposited. In this way, the WAAM process allows for adaptive agency to the robot, so that it can cycle through the layer to be printed with the goal of consistent thermal cycles, rather than just following a pre-planned path.

In an ECS-informed slicing process, the algorithm generates more than just a single toolpath, but a function of parameter space which an adaptive process could dynamically adjust within to accommodate in-process monitoring. In contrast to the single slicing solution provided by typical software, an adaptive slicing algorithm contains a diversity of pathways for control loop adaptation within its planning. In such scenarios, sensor data collected through the ECS framework informs changes to the path planning.

While the current paper focuses on ECS-informed adaptivity, the same strategy could be implemented with a line scanner to monitor and adapt to geometric print height tolerances, where the structure is scanned, and the path planning is adapted accordingly. For example, if the height of the weld layer does not match the intended build volumes, the adaptive path planning algorithm would prescribe remediation paths or other process parameter changes to adjust the build volume back to acceptable heights. In the other direction if the build volume of the weld exceeds the anticipated height the sensor-informed adaptive slicing algorithm integrates this information and remove areas from future toolpaths to continuously mediate between the ideal digital and the intended physical production.

The initial algorithms of this research in dynamic slicing and path planning are based on previous work on adaptivity in incremental point welding (Heimig et al. 2020). Through parametric models and feedback loops between in-line sensors and WAAM controllers, it is possible to create process models which dynamically adjust the path planning based on the ECS framework sensing/measurement units.

As a test case for an ECS-based adaptive slicing strategy, the geometry described in Fig. 9 is used to test the implementation of the concept and its ability to produce support-free overhangs. The image on the left shows a typical planar slicing strategy that relies on supports to enable overhang

production. On the right is shown a dynamically oriented non parallel layer buildup that will be produced using the ECS-based adaptive strategy described above. Initial tests will first develop strategies for non-planar layer deposition as shown in Fig. 9. In this figure, the difference in layer height is illustrated by a series of colored points, equally distributed with a color gradient of red, yellow and green, with red having a layer thickness of 2.15 mm and the points in green representing a layer thickness of 1.15 mm. This print represents the initial overhanging section of the geometry shown in Fig. 10. The starting point of each layer is shifted around the surface of the print resulting in the spiral pattern that can be seen in the points. This is done to reduce the seam buildup along a single section of the structure. The shifting of the layer start points along the curve minimizes the local accumulation of a seam of unwanted material deposition also known as humping which occurs due to the acceleration and deceleration of the robot at the start and end of the layer (Fig. 11).

Subsequent experiments will utilize the ECS concept to dynamically print until thermal thresholds are reached and move to cooler areas of the structure until the previous heat affected zone has cooled sufficiently to receive further deposition. The ECS algorithm will process print areas to dynamically affect heat affected zones as shown in the Fig. 12.

The above process is achieved through a mix of pre-planned design and online adaptation. The pre-planned layer slice is sent to the control units one layer at a time. The middle ware between slicing software and robot execution is designed with a custom skill for dynamic adaptation. This skill executes the welding path while measuring the
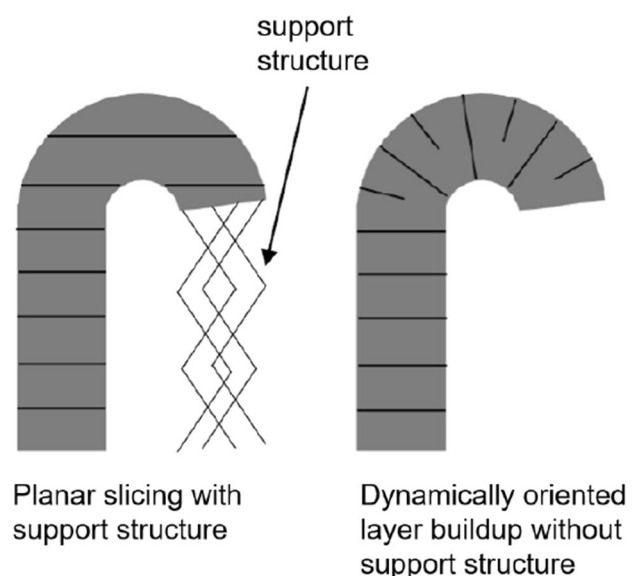

Fig. 9 Planar slicing with support structures and Non-Planar slicing with unsupported overhangs
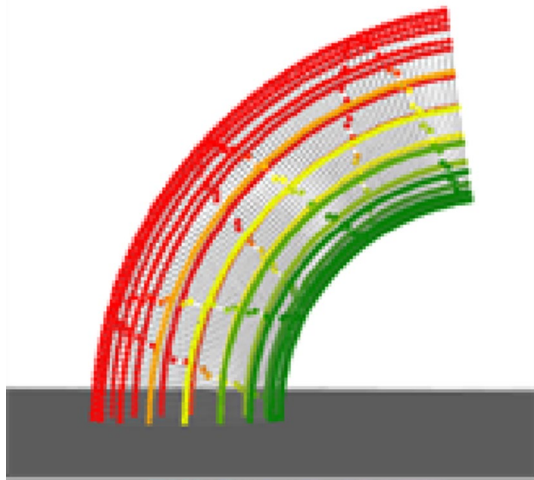
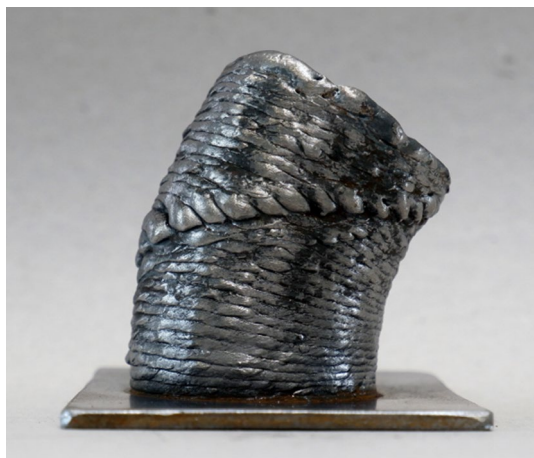**Fig. 10** Non-planar slicing for ECS informed dynamic adaptation

Fig. 11 Non-planar slicing for ECS informed dynamic adaptation

printed the middle ware returns a sync value to the design software and the next layer is pushed through the process. The combination of pre-planned slicing and adaptive middle ware is designed where visual programming environments like Rhino Grasshopper can be combined with custom C# designed robot skills which leverage the custom robot SDK/API interface in combination with KUKA/crc to create extendable programs for integrating customization of adaptive WAAM strategies.

Adaptive path planning algorithms push the limits of current approaches to offline robot programming where pre-defined motions are executed by a robot arm. To build a process model for interconnection between ECS-informed approaches for integrating sensor data into adaptive robotic path planning requires a new system for interconnecting robot, welder and heat sensors. This new approach leverages an IoT cloud-based version of Parametric Robot Control and to connects robotic devices and auxiliary machines such as welding end effectors and sensors in a more industry 4.0 approach to automation. By connecting the toolpath generation to an IoT network it becomes feasible to filter in-line data through the ECS framework and establish adaptive strategies within acceptable parameter spaces. The following section details how the Cloud Remote Control framework forms the foundation for an ECS-based adaptive approach to WAAM path planning.

3.2 IoT enabled systems for online process control

Early methods of robotic fabrication utilized online programming, where positions were physically taught to the robot and then the motion could be repeated for production. Offline programming became a more prevalent way of programming because it allows robot paths to be designed in CAD environments, so that complex robot movements can be planned and simulated before the robot is moved to where they are executed for production. Offline programming often requires robot operators to test simulated movements and adjust the programs to accommodate deviations between the digital simulation environment and the physical production workspace. More advanced robotic cells are able to integrate limited adaptation either by touch off sensing or seam tracking. These adaptations are constrained in their ability to do more than relocate starting positions of robot movements or

temperature and when a threshold is reached the adaptive strategy is engaged. By dynamically adding the already printed path to a list of printed items, the path is removed from the remaining elements to be printed. The robot moves to a cooler area and repeats the process, monitoring when the previously printed area has cooled to a rate where further printing is acceptable. When the layer is fully

Fig. 12 Process diagram for ECS informed adaptive path planning

slight adjustments to simple weld trajectories. This research proposes a more advanced form of ECS informed adaptation in WAAM. To achieve this requires innovative approaches to path planning, as well as IoT enabled systems for online process control and an information model capable of data collection for post process analysis and visualization.

One of the goals of this paper is to propose a connection between the ECS framework and the dynamic adaptivity of the welding parameters. This interconnection is made possible through the connection of the welding power source as an IoT device controllable through the Cyber-Physical Systems such as the Cloud Remote Control framework. This approach builds upon research realized in previous studies by the authors (Lozano and Sharma 2019; al 2020).

This research leverages a new approach to parametric robot programming called Cloud Remote Control (CRC) developed by Robots in Architecture Research. The CRC framework establishes a distributed automation system for extending robotic production into an IoT-enabled network. The aim of CRC is to move automation forward towards a more interconnected approach to automation, allowing for more intelligent and adaptive robotic processes. Through an IoT-enabled infrastructure, CRC extends the KUKA/prc software into a service-based automation solution that can connect closely with the advancing digital infrastructure required the concept of ECS informed adaptation. The benefits of this approach include a more Industry 4.0 flow of information between robot path planning and devices such as the welder and thermal camera. CRC is built on a cloud based, IoT-enabled system of distributed communication protocols. A flow diagram of the CRC process is shown in Fig. 13. The following section details select aspects of the CRC system that are integral to the dynamic WAAM process.

The Main Control Unit (MCU) receives the data from a global server and distributes the commands locally. According to a user-configured description, the MCU forwards the instructions to connected devices through a MQTT publish/subscribe protocol. A standard JSON string allows for consistent communication across connected device types. These commands set the robot and associated machines or end effectors into motion. This method is used both to publish data to the automated devices as well as receive state data back from the automated process, allowing for synchronization of production processes. The state data published back to the cloud allow for the user to monitor the process via a digital twin that can integrate sensor data such as the thermal camera used in the ECS-informed WAAM process.

The described network interface and distributed communication protocol leverages the concepts of Asset Administration Shell (AAS) approaches to Industry 4.0 and the IoT by developing a standard method for describing industrial assets in a digital format. An AAS is a digital twin of an industrial asset, such as a machine, device, or system, and contains information about the physical and functional properties, as well as its behavior and performance. The aim of the AAS is to provide a unified representation of an industrial system for purposes, such as monitoring, control, and optimization. CRC utilizes this structure to create a
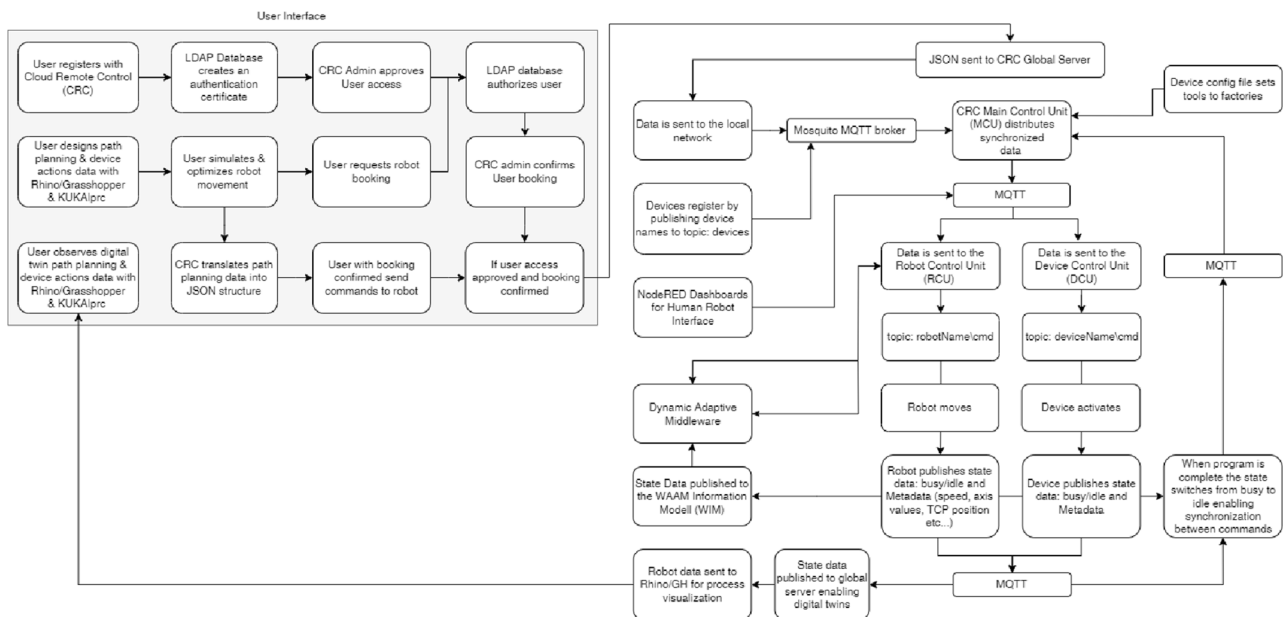

Fig. 13 Structure of cloud remote control Communication

distributed automation system that extends Parametric Robot Control into an IoT-based, globally accessible framework.

The CRC framework is also based on OPC Unified Architecture (OPC UA). This communication protocol is a machine-to-machine standard for automation and the interconnection of IoT devices. This communication protocol is developed for secure communication and data exchange in a platform-independent way. OPC UA is a service-oriented framework that enables the exchange of data across an interconnected system including event-driven data exchange, publish-subscribe models, and security features such as authentication and access control. CRC allows for precise synchronization between IoT-connected components, allowing devices to be integrated in a way that enables adaptation in path planning.

The CRC system is built by connecting devices through the wireless exchange of information using a MQTT publish/subscribe model to send and synchronize messages in a structured JSON format. This allows for the robot to communicate with the welder and the thermal camera via a distributed communication protocol. CRC consists of a cloud-based software architecture, Main Control Units (MCU), Robot Control Units (RCU) and Device Control Units (DCU).

The MCU, shown in Fig. 14, is representative of global access by the user to the CRC network infrastructure of distributed communication. The RCU, shown in Fig. 15, provides local structure for receiving and distributing data amongst the robots, end effectors and IoT enabled machines. The RCU is the software responsible for listening for data from the MCU and returning information back to the network regarding its status. This bi-directional communication allows for the interconnected network to synchronize the sequencing of control commands, ensuring the proper timing of actions across the distributed devices. The RCU
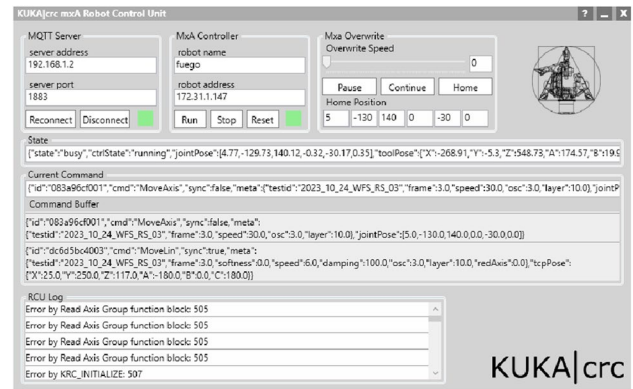

Fig. 15 Cloud remote control—robot control unit (RCU)

exists in multiple forms, ranging from a standalone software in the case of a robot arm, to a DCU which can be encoded Arduino program for opening and closing a gripper or a Python script that translates welder parameter commands into binary for communication with a CAN BUS system. The RCU is extendable with a framework for adding adaptive skills via C#. These skills can then be called from the WAAM algorithm and executed within the ECS informed adaptive concept. These skills can incorporate relative movements and other logic-based control methods. It is this extension to the typical design-to-production workflow that allows for ECS informed adaptation. While initial path planning geometry is designed in the CAD environment, additional skills can be integrated to the robot code. In this way, the path to print is a geometric definition of a layer but the middle ware can add dynamic skill based commands. As an example, one adaptive implementation of this middle ware concept is to create a robot skill so that once the thermal measurement exceeds a certain value, the dynamic method turns off the welder, retracts the robot to a safe distance and finds the next suitable place to begin the next area of welded material deposition.

The purpose of each RCU is to subscribe to its individual topic and communicate program data to the device. Devices and robots are configured to subscribe to "devicename/cmd" and "devicename/ctrl" (mostly used by robots for real time, continuous control). Devices and robots are configured to publish their states to "devicename/cmd" topic. IoT devices (as well as the robot) publish their current state every 50 ms under MQTT topic of "devicename/state".

Node RED interfaces, shown in Fig. 16, are used to interject user driven commands into the pre-programmed process when override controls are required. Information is also displayed to assist the user in process control and monitoring. For the WAAM research, the speed of the robot can be overlaid with information about welder activity and thermal values, providing the operator with a visual representation
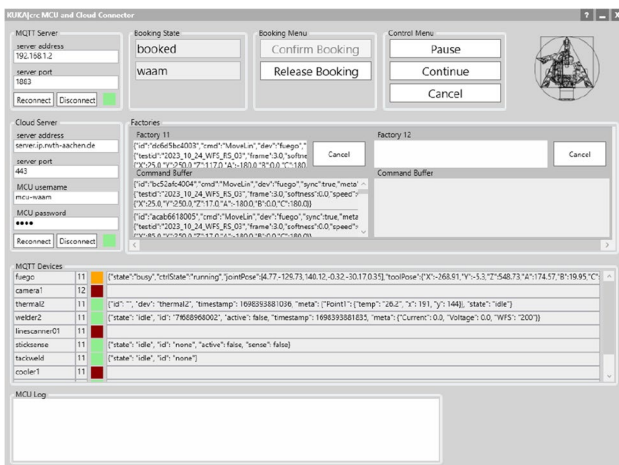

Fig. 14 Cloud remote control—main control unit (MCU)

of the process and allowing easy oversight and actioning of local control if required.

Connected devices receive data by listening for instructions via RCU running on local computers or wireless PCBs. These network interfaces allow for a machine, either a robot or an end effector, to subscribe to the MQTT topic that controls its actions and interprets information according to the type of connected device. The RCU receives the topic information published by the MCU. This information is consistent in its JSON-based format but tailored to the specific device in additional metadata. This enables standardized communication across device types.

While a robot receives path planning information, a gripper will receive high or low signals to control the opening and closing of a gripper. This format is extendable so that another device with more detailed operation parameters, like the IoT-enabled welder used in the WAAM research, can receive user-defined task command information. Once the RCU receives the information the action is set in motion and state data is returned to the network so that the device is booked as busy. When the motion or task is completed, the state data is updated to idle to reflect completion so that subsequent motions can commence according to the planned synchronization sequence. State data can also be updated incrementally, allowing for the robot to publish in process data, for instance its axis values, tool center point (TCP)

position or additional available metadata such as joint torque forces. This device information is published back to the cloud to inform digital twins of the remote robotic process. Process monitoring and digital twins allow remote users or process control algorithms like the ECS informed adaptivity to understand the current state of the automated production and dynamically plan the automated production workflow.

With the MCU managing global communication and the RCU distributing local data and publishing synchronization-based state changes, the robotic process can act as a service for distributed digital production. To build this dynamic adaptive process model, the data from devices and sensors is correlated to the robot movement and stored in an information structure for feature identification and adaptive processing. The CRC framework allows for the integration of sensors enabling them to leverage IoT distributed communication protocols to publish sensor state data back to the cloud. This information is amended to the larger JSON structure so that in process adaptive control models can be created. This is demonstrated in ECS-informed WAAM production where a path planning model is augmented with thermal information for dynamic adaptation. This strategy is used to flag an area of a WAAM 3D print which exceeds temperature thresholds. In initial tests, the robot then dynamically waits for the cool down phase to reach the appropriate level before continuing the weld. In more advanced tests the
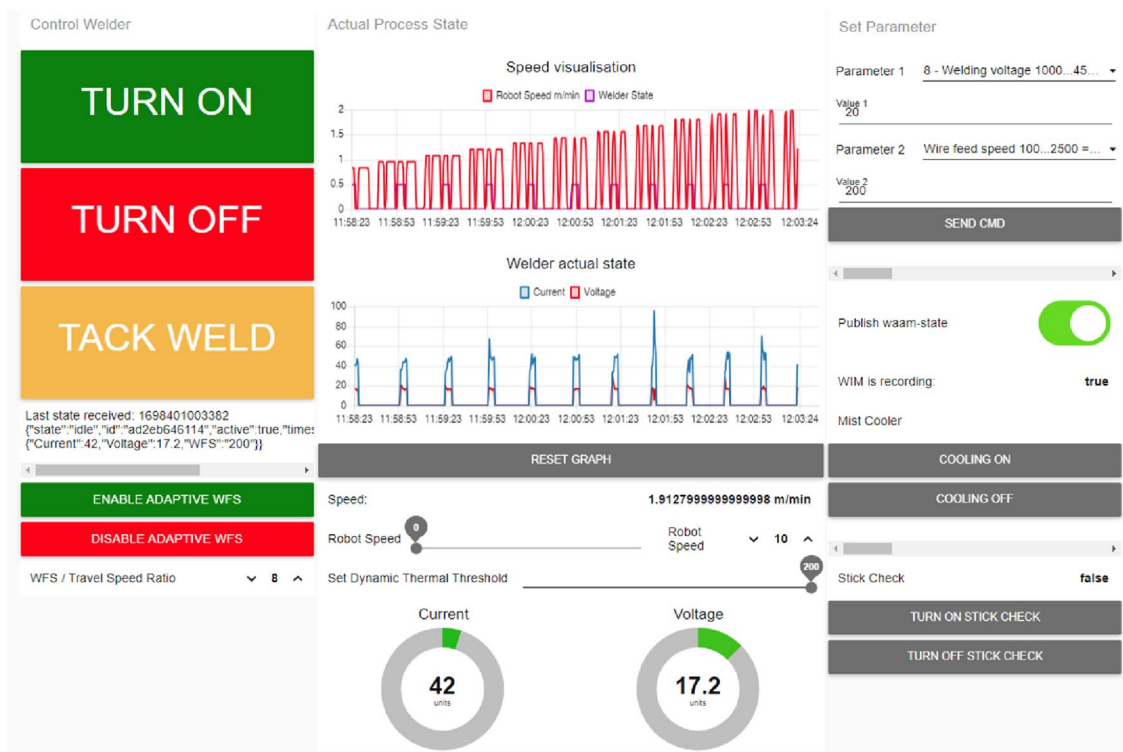

**Fig. 16** Cloud Remote Control—Node RED User Interface

robot is programmed to move to cooler areas of the print and continue welding rather than waiting for a single area to cool. The CRC networked structure enables the amending of metadata with information on thermal measurements, TCP speeds, interpolation-based deviation and timestamps for correlation with video and audio recordings. The extendable structure establishes a communication foundation that can be expanded with plans for line scanners, point cloud and audio information to be next added to the data structure.

This amending of process data into the control model of the automated system enables the creation of further adaptive strategies. Rather than just using the in-process amended metadata for quality control, CRC enables sensor data to be used to inform adaptive processes. A simple implementation of this is to create a state flow where the robot welds until a material temperature is reached, then if the threshold for acceptable heat is exceeded, the process is programmed to save these paths as a heat affected zone. While this area is monitored to assess cooling rates according to the ECS variable, the welder queries the remaining sections of the layer to be printed and finds the next closest area that is ideal for printing on. By tracking cooling rates and dynamically jumping around the print area the WAAM process aims to achieve a more consistent thermal transfer across the build area. The robot is given agency to plan its path to best achieve appropriate cooling times while continuing the WAAM production process.

This dynamic approach to deposition of welded printing material saves time and improves quality by tightly controlling the temperature range that each section of the print receives. More advanced control loops will integrate line scanners for adaptive weld path planning. The amendment of CRC metadata is used to track thermal performance as output from the IoT-enabled Optris thermal camera (Figs. 17, 18). Additional information about the WAAM process can be tracked through amended metadata, including TCP speeds, interpolation-based deviation and timestamped images, video and audio recordings. The structure of the metadata is extendable allowing for an increasing amount of information to be processed for quality control or adaptation.

The amendment of metadata can also be used to control devices during synchronized motions. For example, when the robot executes an interpolated series of commands, it needs to group them between sync flags. This is so that the robot can plan the path between the consecutive number of points, mediating between accuracy and consistency of speed, to smooth out acceleration ramping by moving not precisely to points of travel. This is useful in manufacturing processes like WAAM where speed has a direct impact on the deposition of material. If the robot is moving slower, more material (perhaps unwanted amounts) will be deposited on the build plate. The CRC framework allows for a custom RCU to listen for unique command IDs and update metadata for configured devices without breaking the synchronized

Fig. 17 IoT enabled thermal camera
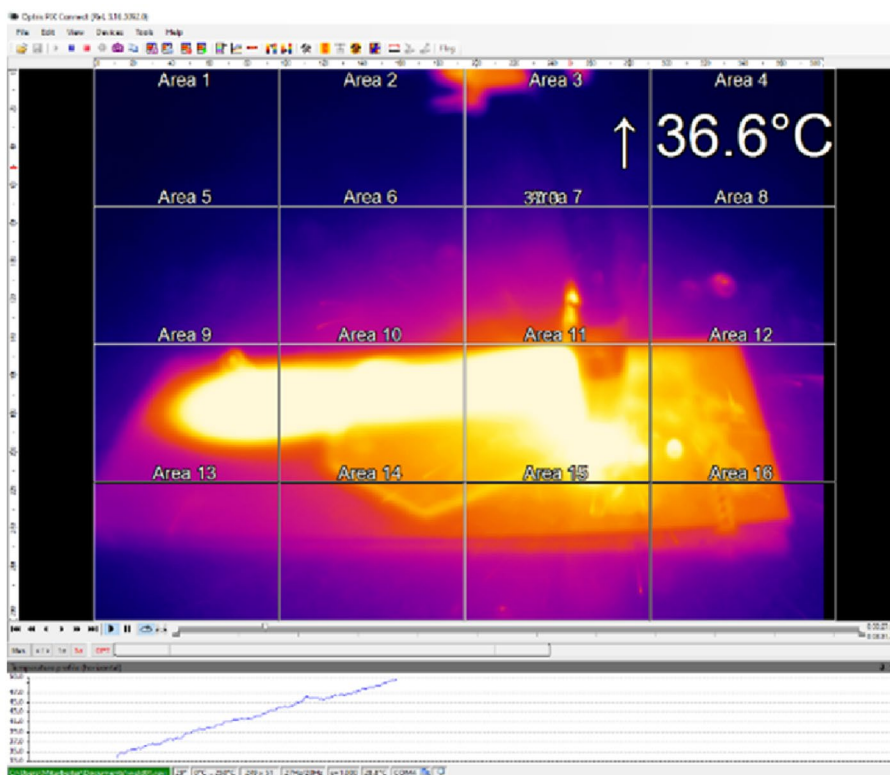
waam/state : msg.payload : Object
▼object
  timestamp: 1699270678723
  ▼fuego: object
    state: "busy"
    ctrlState: "resetting"
    ▼jointPose: array[6]
      0: -0.94
      1: -66.2
      2: 76.65
      3: 0.09
      4: 79.72
      5: -0.5
    ▼toolPose: object
      X: 263.3
      Y: 95.62
      Z: 344.59
      A: -90.68
      B: 0.21
      C: 92.88
    toolVel: 0
    toolId: 6
    baseId: 1
    id: "none"
    confirm: false
    timestamp: 1699029514586
    dev: "fuego"
  ▶meta: object

  ▼welder2: object
      state: "idle"
      id: "none"
      active: false
      timestamp: 1699263478635
    ▼meta: object
        Current: 0
        Voltage: 0
      dev: "welder2"
  ▼thermal2: object
      id: ""
      dev: "thermal2"
      timestamp: 1699263478787
    ▼meta: object
      ▼Point1: object
          temp: "27.1"
          x: 191
          y: 144
      state: "idle"

Fig. 18 CRC metadata

grouping of interpolated groups of movement commands. This has allowed for a dynamic adaptation of wire deposition based on changing TCP speeds during different configurations of robot joint movements. This adaptive strategy enables a dynamic approach to WAAM process modeling.

To enable the dynamic connection between the welding device and overall process control, the CRC system sends machine-specific modified welding parameters, such as wire feed speed, to the welding power source via a fieldbus interface. In this way, both the robot's overall control and the power source can be informed and adapted through the lens of the ECS concept. By making every parameter of the welder accessible to the overall process control system, the adaptive model can change parameters throughout the WAAM production, connecting path planning, and robot speed to changes in amperage, voltage, wire feed speed, and more.

3.3 WAAM information models (WIM)

The development of an ECS-informed adaptive path planning strategy allows the robot to optimize its actions to achieve a more controlled thermal transfer during printing of unsupported overhang structures. The in-process adaptation

is made possible by path planning algorithms that anticipate adaptation, and the CRC framework for distributed communication between robot, welder, and thermal camera. This in-process adaptation is based on the streaming of data between devices. While this data is utilized to inform ECS-based adaptation, the process data is only collected in the limited scope of the sensor-based adaptation. As the collection of this data in the long term will overload the memory of the computational model, a separate database application has been created to collect the information into a post-process analysis model format. The goal of this information model is to collect process data over the long term and make it accessible for adaptation, analysis and visualization. To accomplish this, a connection is built between the CRC data exchange protocol and a SQL database. This WAAM Information Model establishes a framework for capturing process data regarding thermal states, cooling times, welder parameters and robot movement information ranging from speed, TCP position, deviations due to interpolation and timestamps, so that additional data such as images, video or audio of the process can be collated to create a comprehensive database of the process.

Storing the data from the WAAM process in a powerful database is very important as it provides the ability to access data from previous trials, quickly evaluate data and identify potential for improvement. It was decided to store the process information on an SQL server. The database consists of multiple related tables. The "WIM_Tests" table contains test-specific, general information. This includes geometry data and constant settings like wire-speed, robot-speed and other test-specific, general information, which are "set properties" before the execution of WAAM Process. The process data consists of inline information recorded by the robot, welder and thermal camera and can be stored in the "wim.testdata" table. Among other things, temperature, position and image data recorded at short intervals can be found here.

The local server is filled with the data using Grasshopper and several plugins (Fig. 19). This serves as an initial prototype/proof of concept to be later replaced with a more robust python based background application which can more frequently and efficiently be updated with WIM Json string for transmitting to the SQL Server. For the purpose of the WIM prototype, the data is received by KUKA/crc, processed with Slingshot! and finally sent to the server with Ggamagi. On the KUKA/crc side, a connection is established through the MQTT Broker to the MCU. By means of the Subscriber component we listen to the topic "waam/state". This gives us the combined data of the robot, welder and thermal camera. A Python script reads the data and splits it into different outputs. These are passed to the Slingshot! Part. The processing and sending of the data is divided into three sections: one general, one for the WIM_Tests and one for the Testdata table.
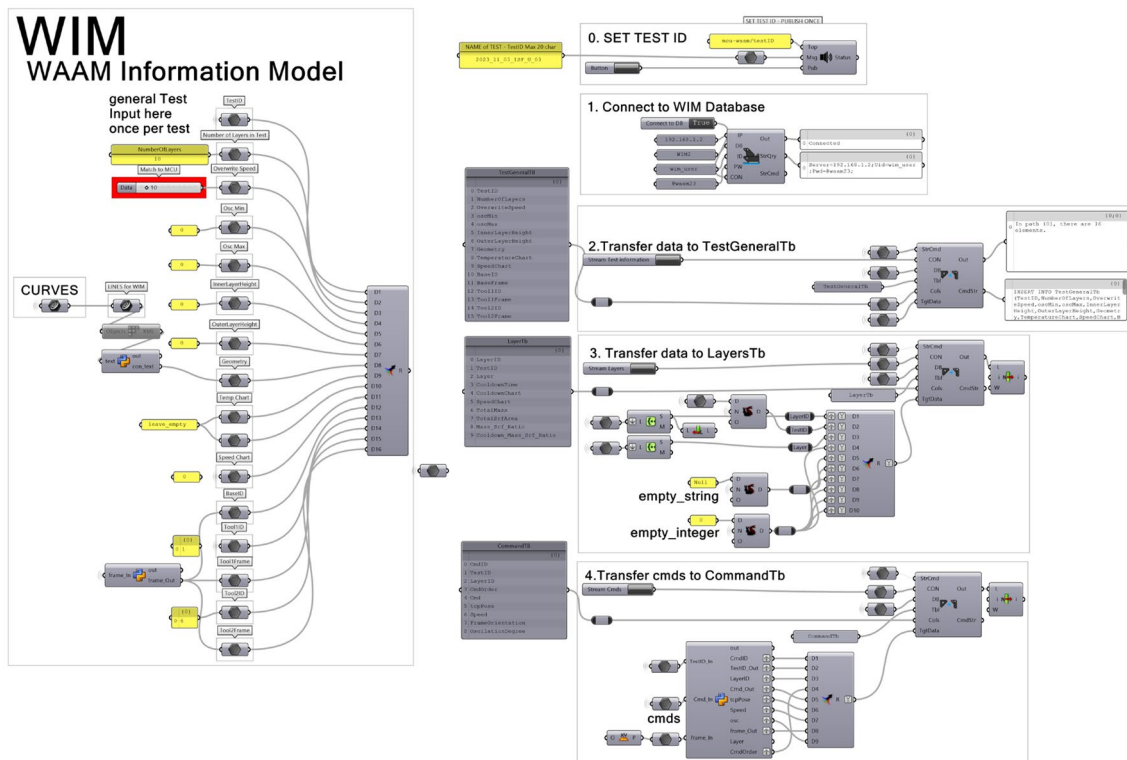
Fig. 19 Grasshopper based communication of data for WAAM Information Model (WIM)

The general part generates the commands that create the database and the tables. In addition, the connection to the server is established. The WIM_Tests data are entered into the fields according to the test and summarized in an insert command. In the third section, the data received by means of KUKA/crc is linked in the correct order and converted into an insert command. Each change of the input causes a new sending of the data, so it is helpful that by KUKA/crc all data can be received at the same time. Through the connection to the MQTT and SQL server, the data is automatically received and forwarded to the WIM SQL Database (Fig. 20).

In addition to writing, it is also possible to pull the data back into Grasshopper, rebuild visualization models and evaluate results computationally. For this purpose, SQL queries are sent to the server. The received information can be used, for example, to clearly display the measured temperatures and velocities graphically. Likewise, a specific viewing of individual data sets is possible. In addition to the numerical data, the image of the thermal camera is also displayed.

Through the lens of the ECS, it becomes possible to explore new approaches to adaptation of WAAM production. While traditional welding specifications fix the parameters of the welder and the robot, a dynamic approach has the potential to push the WAAM process into new areas of performance. The goal is to enable not only more high-quality production but extend the usable space of WAAM

into areas that prove too challenging for static processes. Empowered with a new framework for adaptivity and ECS optimization, this approach seeks to bring WAAM beyond pre-production and into aspects of construction that were previously not possible. If this new approach can extend the reach of the WAAM process into on-site construction and infrastructure repair, a new avenue for application scenarios becomes possible. The goal of this paper is to establish the foundation for researching such an approach and framing future experiments in this context. The following conclusion summarizes this goal and provides an outlook towards future research objectives.

4 Conclusion and outlook

This research paper examines the WAAM process to develop the novel concept of an Equivalent Contact Surface (ECS) and build a foundation for dynamic path planning to achieve a greater control over thermal dynamics and enable the production of support free overhanging structures. An explanation of the ECS concept is detailed and used to expand upon ideas for dynamic path planning algorithms, in-line process adaptations and the creation of information models.

Adaptive control algorithms which monitor process parameters create a wealth of information. Further WAAM

Fig. 20 SQL database for WAAM Information Model (WIM)

testing will research into the parameter space that defines the ECS concept and collect data from different sources both digital and physical, integrating these into the WAAM Information Model (WIM) for process analysis and development of a deeper understanding of the ECS concept. Initial data from geometry models and path planning will combine with live monitoring of robot status and welding process to create this database of both in-process adaptation and post-process analysis. To research the parameter space of the ECS, the structure of the Cloud Remote Control software will be further integrated into the WAAM process and Information Model to detail the method for adding additional sensor inputs and data points. The WIM will next incorporate the synchronization of timestamped images, video and later audio recordings for process analysis. By integrating the CRC distributed communication protocol as an extendable information protocol this research enables the creation of a WAAM process model which can incorporate an increasing number of data sources. Special thanks to, Emre Ergin, Görkem Ertemli, Heinrich Knitt and Dr. Sven Stumm from Robots in Architecture Research, for their collaboration in support of this projects technical development.

Future studies will examine various welding and robotic parameters that shall be investigated on their influence on the heat accumulation, distribution, and dissipation within the specimen. The influence of these parameters will continue to inform the ECS auxiliary variable. After modeling the ECS the usable parameter space regarding the welding position and the deposition rate shall be determined and the mechanical-technological properties of the welds in terms of anisotropy will be investigated. Adaptive strategies described in this research will continue to be developed, tested, and documented.

Further measuring systems that are potentially to be implemented include a quotient pyrometer, thermocouples for temperature measurement, a laser line scanner for layer height measurement, and a 3D scanner to compare the buildup specimen to the initial CAD model for accuracy determination. Parameter tests will be conducted with welds done on a base plate with different angles to investigate the gravitational influence. The specimens that are planned to be welded are thin walled and use different geometrical forms that vary in volume and surface area for different heat capacities and dissipation rates. The different geometric forms allow the investigation of various welding angles under gravitational influence. The influence of these parameters is then summarized in an auxiliary variable called the ECS. After a more detailed modeling of the ECS, the usable parameter space will inform adaptive path planning and investigated in terms of the mechanical-technological properties and anisotropy or the printed WAAM structure. Through documentation of the ECS adaptive path planning framework, this research opens the development of this process model to further scientific inquiry and innovation.

Declarations

Conflict of interest On behalf of all authors, the corresponding author states that there is no conflict of interest.

References

al SM (2020) Study on weld seam geometry control for connected gas metal arc welding systems. In: 2020 17th international conference on ubiquitous robots UR, pp. 373–379

Anzehaee MM, Haeri M (2011) Welding current and arc voltage control in a gmaw process using armarkov based mpc. Control Eng Pract 19: 1408–1422 https://doi.org/10.1016/j.conengprac.2011.07.015

Bingham N, Fry J (2010) Regression. Linear Models Stati. https://doi.org/10.1007/978-1-84882-969-5

Chen S, Zhang Y, Feng, Z (2018) Transactions on Intelligent Welding Manufacturing

DIN German Institute for Standardization: Additive manufacturing—General principles—Part 2: overview of process categories and feedstock (ISO 17296-2:2015) (2016)

Dinovitzer M, Chen X, Laliberte J, Huang X, Frei H (2019) Effect of wire and arc additive manufacturing (waam) process parameters on bead geometry and microstructure. Additive Manuf 26:138–146. https://doi.org/10.1016/j.addma.2018.12.013

Duraisamy R, Kumar SM, Kannan AR, Shanmugam NS, Sankaranarayanasamy K (2021) Fatigue behavior of austenitic stainless steel 347 fabricated via wire arc additive manufacturing. J Materi Eng Perform 30:6844–6850. https://doi.org/10.1007/s11665-021-06033-3

Geng R, Du J, Wei Z, Xu S, Ma N (2021) Modelling and experimental observation of the deposition geometry and microstructure evolution of aluminum alloy fabricated by wire-arc additive manufacturing. J Manuf Process 64:369–378. https://doi.org/10.1016/j.jmapro.2021.01.037

Ghaffari M, Vahedi Nemani A, Rafieazad M, Nasiri A (2019) Effect of solidification defects and haz softening on the anisotropic mechanical properties of a wire arc additive-manufactured low-carbon low-alloy steel part. JOM 71:4215–4224. https://doi.org/10.1007/s11837-019-03773-5

Gurcik T, KOVANDA K, ROHAN P (2019) In influence of shielding gas on geometrical quality of waam technology. 28th International conference on metallurgy and materials, 715–721 22-24 May . https://doi.org/10.1016/j.addma.2018.12.013

Hallam JM, Kissinger T, Charrett TOH, Tatam RP (2022) In-process range-resolved interferometric (rri) 3d layer height measurements for wire + arc additive manufacturing (waam). Meas Sci Technol 33:44002. https://doi.org/10.1088/1361-6501/ac440e

Heimig T, Kerber E, Stumm S, Mann S, Reisgen U, Brell-Cokcan S (2020) Towards robotic steel construction through adaptive incremental point welding. Constr Robot 4:49–60. https://doi.org/10.1007/s41693-019-00026-4.Bibliography

JSRSMSSO et al.: Quantitative Evaluation of SPH in TIG Spot Welding. Comp. Part. Mech, (2022). https://doi.org/10.1007/s40571-022-00465-x

Jurié I, Garašié I, Bušié M, Kožuh Z (2019) Influence of shielding gas composition on structure and mechanical properties of wire and arc additive manufactured inconel 625. JOM 71:703–708. https://doi.org/10.1007/s11837-018-3151-2

Lee SH (2020) Optimization of cold metal transfer-based wire arc additive manufacturing processes using gaussian process regression. Metals 10:461. https://doi.org/10.3390/met10040461

Lopez A, Bacelar R, Pires I, Santos T, Quintino, L (2017) Mapping of non-destructive techniques for inspection of wire and arc additive manufacturing. In: Proceedings of the 7th international conference on mechanics and materials in design

Lozano URSMLOP, Sharma R (2019) Study on workpiece and welding torch height control for polydirectional waam by means of image processing. In: 2019 IEEE 15th international conference on automation science and engineering (CASE, pp. 6–11 https://doi.org/10.1109/COASE.2019.8843076

Pan Z, Ding D, Wu B, Cuiuri D, Li H, Norrish J (2018) Arc welding processes for additive manufacturing: a review. In: Springer (ed.) Transactions on Intelligent Welding Manufacturing and Chen, pp. 3–24

Penney JJ, Hamel WR (2019) Using non-gravity aligned welding in large scale additive metals manufacturing for building complex parts. In: Proceedings of the 30th Annual International Solid Freeform Fabrication Symposium

Reisgen U, Sharma R, Mann S, Oster L (2020) Increasing the manufacturing efficiency of waam by advanced cooling strategies. Weld World 64:1409–1416. https://doi.org/10.1007/s40194-020-00930-2

Richter A, Scheck M, Gehling T, Bohn C, Wesling V, Rembe, C (2021) Erfassung geometrischer daten des schmelzbades zur regelung eines waam-prozesses. tm - technisches messen **88**. https://doi.org/10.1515/teme-2021-0072

Schroepfer D, Scharf-Wildenhain R, Haelsig A, Wandtke K, Kromm A, Kannengiesser T (2021)Process-related influences and correlations in wire arc additive manufacturing of high-strength steels. Ser.: Mater 1147, 12002 https://doi.org/10.1088/1757-899X/1147/1/012002

Shassere B, Nycz A, Noakes M, Masuo C, Sridharan N (2019) Correlation of microstructure and mechanical properties of metal big area additive manufacturing. Appl Sci 9:787. https://doi.org/10.3390/app9040787

Shi J, Li F, Chen S, Zhao Y, Tian H (2018) Effect of in-process active cooling on forming quality and efficiency of tandem gmaw–based additive manufacturing. Int J Adv Manuf Technol

Su C, Chen X (2019) Effect of depositing torch angle on the first layer of wire arc additive manufacture using cold metal transfer (cmt). IR 46, 259–266 https://doi.org/10.1108/IR-11-2018-0233

Syed AK, Zhang X, Davis AE, Kennedy JR, Martina F, Ding J, Williams S, Prangnell PB (2021) Effect of deposition strategies on fatigue crack growth behaviour of wire + arc additive manufactured titanium alloy ti-6al-4v. Mater Sci Eng 814(14119):4. https://doi.org/10.1016/j.msea.2021.141194

Tang F, Luo Y, Cai Y, Yang S, Zhang F, Peng Y (2022) Arc length identification based on arc acoustic signals in gta-waam process. Int J Adv Manuf Technol 118:1553–1563. https://doi.org/10.1007/s00170-021-08044-9

Technology of Materials Standards Committee (2017) Additive manufacturing—General principles—Fundamentals and vocabulary (ISO/ASTM 52900:2021)

van Le T, Mai DS, Hoang QH (2020) study on wire and arc additive manufacturing of low-carbon steel components: process stability, microstructural and mechanical properties. J Braz. Soc. Mech. Sci. Eng **42**https://doi.org/10.1007/s40430-020-02567-0

Wächter M, Leicher M, Hupka M, Leistner C, Masendorf L, Treutler K, Kamper S, Esderts A, Wesling V, Hartmann S (2020) Monotonic and fatigue properties of steel material manufactured by wire arc additive manufacturing. Appl Sci 10:5238. https://doi.org/10.3390/app10155238

Wang X, Wang A, Li Y (2020) An online surface height measurement method for gtaw-based additive manufacturing. Weld World 64:11–20. https://doi.org/10.1007/s40194-019-00813-1

Wang Z, Zimmer-Chevret S, Léonard F, Abba G (2022) Improvement strategy for the geometric accuracy of bead's beginning and end parts in wire-arc additive manufacturing (waam). Int J Adv Manuf Technol 118:2139–2151. https://doi.org/10.1007/s00170-021-08037-8

Wu B, Pan Z, van Duin S, Li H (2019) Thermal behavior in wire arc additive manufacturing: Characteristics, effects and control. In: Transactions on intelligent welding manufacturing, pp. 3–18. Springer, Springer Singapore

Xu F, Dhokia V, Colegrove P, McAndrew A, Williams S, Henstridge A, Newman ST (2018) Realisation of a multi-sensor framework for process monitoring of the wire arc additive manufacturing in producing ti-6al-4v parts. Int J Comput Integrated Manuf 31:785–798. https://doi.org/10.1080/0951192X.2018.1466395

Yaseer A, Chen H, Zhang B (2021) Predicting layer roughness with weaving path in robotic wire arc additive manufacturing using multilayer perceptron. In: 2021 IEEE 11th annual international conference on CYBER technology in automation, pp. 27–31. Control, Jiaxing, China

Yildiz AS, Davut K, Koc B (2020) Yilmaz: Wire arc additive manufacturing of high-strength low alloy steels: study of process parameters and their influence on the bead geometry and mechanical

characteristics. Int J Adv Manuf Technol 108:3391–3404. https://doi.org/10.1007/s00170-020-05482-9

Zhang C, Qiu Z, Zhu H, Wang Z, Muránsky O, Ionescu M, Pan Z, Xi J, Li H (2022) On the effect of heat input and interpass temperature on the performance of inconel 625 alloy deposited using wire arc additive manufacturing-cold metal transfer process. Metals 12:46. https://doi.org/10.3390/met12010046

Zhao D, Long D, Niu T, Zhang T, Hu X, Liu Y (2022) Effect of Mg Loss and Microstructure on Anisotropy of 5356 Wire Arc Additive Manufacturing. J. of Materi Eng and Perform, https://doi.org/10.1007/s11665-022-06802-8